Available online at www.sciencedirect.com

ScienceDirect

Scripta Materialia 77 (2014) 29–32

Scripta MATERIALIA

www.elsevier.com/locate/scriptamat

Penetration of protective chromia scales by carbon

David J. Young,[a,*] Thuan Dinh Nguyen,[a] Peter Felfer,[b] Jianqiang Zhang[a] and Julie M. Cairney[b]

[a] *School of Materials Science and Engineering, University of New South Wales, NSW 2052, Sydney, Australia*
[b] *Aerospace, Mechanical and Mechatronic Engineering, Australian Centre for Microscopy and Microanalysis, The University of Sydney, NSW 2006, Sydney, Australia*

Received 7 November 2013; revised 8 January 2014; accepted 10 January 2014
Available online 15 January 2014

Model Fe–20Cr (wt.%) alloy, exposed to Ar–20CO_2 at 650 °C, formed a protective Cr_2O_3 scale, but nonetheless carburized. Atom probe analysis shows that carbon penetrates the scale via oxide grain boundaries.
© 2014 Acta Materialia Inc. Published by Elsevier Ltd. All rights reserved.

Keywords: Carbon; Cr_2O_3; Penetration; Oxidation

New technologies for reduced CO_2 emissions, such as oxyfuel-fired [1] and solar thermal [2] power generation, involve handling hot CO_2. Heat-resisting alloys appropriate for these temperatures resist corrosion by forming thin, protective Cr_2O_3 scales. Although successful in withstanding heated air or oxygen, this design fails to resist CO_2, in which case an iron-rich oxide scale develops [3–12], leading to unacceptable alloy consumption rates.

This failure is associated with internal carburization of the alloys beneath their oxide scales. At first sight, this is surprising, as carbon activities required to form the observed $(Cr,Fe)_{23}C_6$ precipitates are much higher than those of gaseous CO_2. Thus an Fe–9Cr alloy carburizes at 650 °C in Ar–20CO_2 at 1 atm, where the carbon activity $a_C = 1.6 \times 10^{-15}$, although a value of $a_C \geqslant 8.5 \times 10^{-4}$ is required to stabilize the carbide [13,14].

This is explained by equilibration at the scale–alloy interface, where the oxygen potential is controlled by the reaction

$$M + \frac{\upsilon}{2}O_2 = MO_\upsilon \quad (1)$$

If carbon is present, the equilibrium

$$CO_2 = CO + \frac{1}{2}O_2 \quad (2)$$

controls the CO/CO_2 activity ratio. For a given total pressure, a_C is then set through the Boudouard reaction

$$2CO = CO_2 + C \quad (3)$$

This mechanism correctly predicts [8] carbide volume fraction and carburization rate beneath an iron-rich oxide scale on Fe–9Cr exposed to Ar–20CO_2 at 650 °C. In this gas, an Fe–20Cr alloy forms a thin scale of apparently pure Cr_2O_3, resisting iron-rich oxide formation for up to 240 h at 818 °C [3]. Nonetheless, this alloy carburizes internally beneath its chromia scale.

How carbon penetrates an otherwise protective chromia scale is an important question: the process is associated with premature alloy destruction. Carbon is thought not to dissolve in the oxide [15], and lattice diffusion is therefore unimportant. Instead, carbon must penetrate the scale via extended defects. Gaseous diffusion within macrocracks or pores cannot contribute, as oxygen and carbon activities beneath the scale would then be similar to those of the external gas, and carburization would be thermodynamically impossible.

Permeation of molecular species via nanoscale pores [15] and oxide grain boundaries [16,17] have been suggested, but direct evidence was lacking. The present paper describes microstructural differences in Cr_2O_3 scales grown in CO_2, and the location of carbon within them.

* Corresponding author. Tel.: +61 2 9385 4322; fax: +61 2 9385 5956; e-mail: d.young@unsw.edu.au

1359-6462/$ - see front matter © 2014 Acta Materialia Inc. Published by Elsevier Ltd. All rights reserved.
http://dx.doi.org/10.1016/j.scriptamat.2014.01.009

A model alloy Fe–20Cr was produced by argon arc melting high-purity metals (Cr 99.995%, Fe 99.97%) using non-consumable electrodes. Subsequent annealing at 1150 °C under flowing Ar–5H_2 for 50 h, produced coarse-grained (~400 μm) ferrite. The composition was chemically analysed as 20.4 wt.% Cr and 290 ppmm C. Rectangular specimens cut from the annealed alloy were ground to a 1200 grit surface finish, and ultrasonically cleaned in ethanol before use. The resulting subsurface deformation promotes alloy diffusion and Cr-rich oxide formation [18].

Alloy specimens were inserted into flowing mixtures of either Ar–20CO_2 or Ar–20O_2 preheated to 650 °C at a pressure of 1 atm. The resulting scales and subsurface reaction products were characterized by metallography, scanning electron microscopy (SEM), transmission electron microscopy (TEM) and atom probe tomography (APT).

Cross-sectional views of the alloy reaction products in Figure 1 show that reaction in each of CO_2 and oxygen produced external scales of Cr_2O_3. Etching with modified glyceregia (10 ml glycerine + 6 ml HCl + 3 ml HNO_3) has revealed internal carbides on alloy grain boundaries after exposure to CO_2. These were identified by selected area electron diffraction (SAD) in the TEM as face-centred cubic $M_{23}C_6$ (Fig. 1a).

Internal carbide precipitation depth increased with exposure time in Ar–20CO_2: no carbide was observed after 20 h, but precipitation reached depths of 175 μm after 70 h and 630 μm after 120 h, at which point the alloy specimen thickness had been penetrated. This suggests that, after a short period, carbon penetrates the chromia scale and continues to pass through it into the alloy. A two-stage experiment confirmed this conclusion. A single alloy specimen was exposed in Ar–20O_2 for 24 h, the gas supply switched without change in temperature and exposure continued in Ar–20CO_2 for a further 70 h. The results in Figure 1(c) demonstrate clearly that carbon species from the gas passed through the pre-existing chromia scale, carburizing the alloy beneath.

An understanding of the way in which carbon penetrates the Cr_2O_3 scale requires knowledge of its properties. Examination by TEM revealed the scale microstructures shown in Figure 2, along with the corresponding diffraction patterns. All layers were Cr_2O_3. Table 1 lists oxide grain sizes measured from the images shown, and layer thicknesses, X, measured from a series of SEM cross-sectional views. Grain sizes developed in CO_2 are significantly smaller than those grown in oxygen. Assuming scale growth was controlled by diffusion, then the kinetics of thickening are described by:

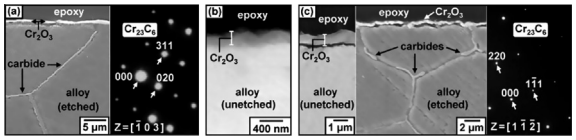

Figure 1. SEM views of reaction product cross-sections: (a) after 120 h in Ar–20CO_2; (b) after 24 h in Ar–20O_2; (c) after 24 h in Ar–20O_2 followed by 70 h in Ar–20CO_2. SAD patterns for internal carbides accompany (a) and (c).

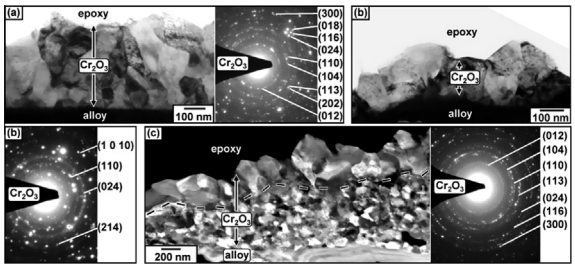

Figure 2. (a, b) TEM bright-field images and SAD patterns of Cr_2O_3 scale cross-sections after reactions: (a) Ar–20CO_2 for 120 h and (b) Ar–20O_2 for 24 h. (c) STEM dark-field image and SAD pattern of the scale produced by reaction with Ar–20O_2 (24 h) then with Ar–20CO_2 (70 h).

$$X_2 = 2k_p t \tag{4}$$

where t denotes time and k_p is the parabolic rate constant. Values of $k_p = 5.8 \times 10^{-15}$ and 2.3×10^{-15} $cm^2\ s^{-1}$ in CO_2 and oxygen, respectively, are estimated from these values of X. As diffusion in Cr_2O_3 is predominantly a grain boundary phenomenon at these temperatures [19], the observation of more numerous grain boundaries in the scale grown in CO_2 is consistent with its faster growth.

Two-stage reaction in oxygen followed by CO_2 produced the two-layered scale seen in the STEM dark-field image of Figure 2(c). Both layers were identified by SAD as Cr_2O_3. As seen in Table 1, the outer layer resulting from the two-stage reaction corresponds approximately in thickness, X_o, and grain size to the single layer formed in the first stage of reaction in oxygen alone. Evidently the second (CO_2) stage of reaction produced fine-grained oxide beneath the first-formed layer, reflecting the inward diffusion of oxidant. Using the measured inner layer thickness in Eq. (1) leads to the estimate $k_p = 5.2 \times 10^{-15}$ $cm^2\ s^{-1}$, assuming inner layer growth commenced when the reaction gas was changed from oxygen to CO_2. This value of k_p is almost the same as that found for scaling during the reaction with CO_2 alone. Measurements of X_O after the two-stage experiment were subject to substantial scatter, and a small amount of additional outer layer growth during the CO_2 exposure is possible.

Tracer diffusion experiments [20], show that chromia scales grow in oxygen at 1050 °C by outward metal diffusion, but grow mainly by inward oxidant transport in H_2/H_2O gas. A similar pattern of behaviour is apparent at the lower temperature of 650 °C used here, where the use of CO_2 leads to production of finer oxide grains, faster scaling and inward scale growth. Obviously, these changes would not result if the mobile species within the scale were simply oxygen ions in both cases. Since, moreover, the CO_2 reaction leads to carburization as well as oxidation, inward transport of a compound species such as molecular CO_2 is a reasonable hypothesis. Since the presence of carbon alters the oxide grain size (Fig. 2), it is also likely that the carbon interacts with grain boundaries. The latter hypothesis was tested using APT of a scale grown in Ar–20CO_2.

Data were collected from several regions in the oxide scale near the intersection of a carbide decorated alloy grain boundary with its surface. For this purpose, a

Download English Version:

https://daneshyari.com/en/article/7913565

Download Persian Version:

https://daneshyari.com/article/7913565

Daneshyari.com